

Article

Xylan Deconstruction by Thermophilic *Thermoanaerobacterium bryantii* Hemicellulases Is Stimulated by Two Oxidoreductases

Zhuolin Yi ^{1,2,†}, Xiaoyun Su ^{1,2,†}, Abigail E. Asangba ^{1,2,3,†} , Ahmed M. Abdel-Hamid ^{2,4} ,
Siddhartha Chakraborty ^{2,5}, Dylan Dodd ^{1,2,5}, Peter G. Stroot ³, Roderick I. Mackie ^{1,2,3} and Isaac Cann ^{1,2,3,5,*}

¹ Energy Biosciences Institute, University of Illinois, 1206 West Gregory Drive, Urbana, IL 61801, USA; yizl1982@hotmail.com (Z.Y.); suxiaoyun@caas.cn (X.S.); Asangba.Abigail@mayo.edu (A.E.A.); ddodd2@stanford.edu (D.D.); r-mackie@illinois.edu (R.I.M.)

² Carl R. Woese Institute for Genomic Biology, University of Illinois, 1206 West Gregory Drive, Urbana, IL 61801, USA; ahetta@illinois.edu (A.M.A.-H.); sc99@illinois.edu (S.C.)

³ Department of Animal Sciences, University of Illinois, 1207 West Gregory Drive, Urbana, IL 61801, USA; pgstroot@gmail.com

⁴ Department of Botany and Microbiology, Faculty of Science, Minia University, 1207 West Gregory Drive, El-Mina 61519, Egypt

⁵ Department of Microbiology, University of Illinois, Urbana, IL 61801, USA

* Correspondence: icann@illinois.edu; Tel.: +1-217-333-2090

† These authors contributed equally to this work.

Abstract: *Thermoanaerobacterium bryantii* strain mel9^T is a thermophilic bacterium isolated from a waste pile of a corn-canning factory. The genome of *T. bryantii* mel9^T was sequenced and a hemicellulase gene cluster was identified. The cluster encodes seven putative enzymes, which are likely an endoxylanase, an α -glucuronidase, two oxidoreductases, two β -xylosidases, and one acetyl xylan esterase. These genes were designated *tbxyn10A*, *tbagu67A*, *tbheoA*, *tbheoB*, *tbxyl52A*, *tbxyl39A*, and *tbaxe1A*, respectively. Only TbXyn10A released reducing sugars from birchwood xylan, as shown by thin-layer chromatography analysis. The five components of the hemicellulase cluster (TbXyn10A, TbXyl39A, TbXyl52A, TbAgu67A, and TbAxe1A) functioned in synergy to hydrolyze birchwood xylan. Surprisingly, the two putative oxidoreductases increased the enzymatic activities of the gene products from the xylanolytic gene cluster in the presence of NADH and manganese ions. The two oxidoreductases were therefore named Hemicellulase-Enhancing Oxidoreductases (HEOs). All seven enzymes were thermophilic and acted in synergy to degrade xylans at 60 °C. Except for TbXyn10A, the other enzymes encoded by the gene cluster were conserved with high amino acid identities (85–100%) in three other *Thermoanaerobacterium* species. The conservation of the gene cluster is, therefore, suggestive of an important role of these enzymes in xylan degradation by these bacteria. The mechanism for enhancement of hemicellulose degradation by the HEOs is under investigation. It is anticipated, however, that the discovery of these new actors in hemicellulose deconstruction will have a significant impact on plant cell wall deconstruction in the biofuel industry.

Keywords: hemicellulase-enhancing oxidoreductase; *Thermoanaerobacterium bryantii*; hemicellulase gene cluster; biofuel; thermostability; xylan



Citation: Yi, Z.; Su, X.; Asangba, A.E.; Abdel-Hamid, A.M.; Chakraborty, S.; Dodd, D.; Stroot, P.G.; Mackie, R.I.; Cann, I. Xylan Deconstruction by Thermophilic *Thermoanaerobacterium bryantii* Hemicellulases Is Stimulated by Two Oxidoreductases. *Catalysts* **2022**, *12*, 182. <https://doi.org/10.3390/catal12020182>

Academic Editor: Vincenzo Vaiano

Received: 28 December 2021

Accepted: 27 January 2022

Published: 31 January 2022

Publisher's Note: MDPI stays neutral with regard to jurisdictional claims in published maps and institutional affiliations.



Copyright: © 2022 by the authors. Licensee MDPI, Basel, Switzerland. This article is an open access article distributed under the terms and conditions of the Creative Commons Attribution (CC BY) license (<https://creativecommons.org/licenses/by/4.0/>).

1. Introduction

Hemicellulose represents the second most abundant component in plant biomass. Efficient degradation of hemicellulose is critical for economical utilization of the plant cell wall polysaccharides in biofuel production. A major component of hemicellulose is heterogeneous xylan, which contains linear xylose-configured backbones decorated with arabinofuranosyl, glucuronyl, feruloyl, and acetyl group side chains. Therefore, the complete degradation of heterogeneous xylan into simple sugars requires the synergistic action of a set of hemicellulases [1]. In a coordinated process, endo-1,4- β -xylanases (EC

3.2.1.8) hydrolyze the xylan backbone into xylooligosaccharides, β -xylosidases (EC 3.2.1.37) cleave the xylooligosaccharides into xylose, and the accessory hemicellulases such as α -glucuronidases (EC 3.2.1.139), α -L-arabinofuranosidases (EC 3.2.1.55), and acetyl xylan esterases (EC 3.1.1.72) catalyze the removal of the side chains.

Thermoanaerobacterium bryantii strain mel9^T is a thermophilic bacterium isolated from a waste pile of a corn-canning factory. The bacterium exhibits a maximum growth temperature of 69 °C. Degradation of hemicellulose by thermostable enzymes provides several industrial advantages, including accelerated reaction rate, solubility, better enzyme accessibility to the substrate, resistance to denaturing solvents, and higher robustness under harsh conditions [2]. *T. bryantii* is able to utilize a wide range of carbohydrates, including xylan. The genome of *T. bryantii* mel9^T has been partially sequenced (Cann et al., unpublished data). Via a homology search, five hemicellulase genes in a gene cluster in the *T. bryantii* mel9^T genome were identified. The genes encoded five putative hemicellulases, including an endo-xylanase, two β -xylosidases, one α -glucuronidase, and one acetyl xylan esterase. Therefore, the products of the gene cluster were predicted to be involved in hemicellulose degradation. The gene products were therefore characterized for their biochemical properties with an emphasis on xylan degradation. Interestingly, two genes encoding putative oxidoreductases with unknown functions were also identified in this gene cluster. Different from the putative hemicellulases, the function of the putative oxidoreductases could not be predicted, and therefore their role in hemicellulose degradation was unclear. Several enzymes, such as members of the previously classified glycoside hydrolase (GH) 61 family, which employ an oxidative hydrolysis mechanism, have been shown to be involved in the degradation of the major plant polysaccharide cellulose [3–7]. Therefore, an oxidation reaction can be critical in plant cell wall polysaccharide deconstruction. In this paper, we biochemically characterized the five hemicellulases. Importantly, we expressed and purified the two associated oxidoreductases to determine their effect on the hydrolytic activity of the *T. bryantii* hemicellulose-degrading enzymes.

2. Results

2.1. Isolation and Characterization of the *T. bryantii* mel9^T Strain

From a waste pile of a canning factory in Hoopston, IL, USA, we isolated a thermophilic bacterium mel9^T. The cells of the isolated strain mel9^T were straight rods and occurred singly or in pairs. Motility was by peritrichously arranged flagella (Figure 1). Strain mel9^T cells were stained Gram-negative. However, thin sections showed a Gram-positive ultrastructure. The cells grew at pH 5.0–8.0, with the growth optimum at pH 6.8–7.0. The optimum temperature for growth was 62–65 °C, at pH 6.8, and the upper and lower temperature limits of growth were 69 and 45 °C, respectively (Supplemental Table S1). The end products of glucose fermentation were acetate, butyrate, ethanol, butanol, CO₂, and H₂. Strain mel9^T did not reduce thiosulfate to sulfide. Furthermore, the bacterium reduced neither sulfate nor sulfite. Phylogenetic analysis based on the 16S rRNA gene sequence indicated that strain mel9^T clusters within the low G + C phylum and is closely related to *Thermoanaerobacterium thermosaccharolyticum* (Figure 2). However, the DNA–DNA hybridization for the two strains was only 65.7%. A DNA–DNA hybridization value less than or equal to 70% is considered as an indication that an organism belongs to a different species than the strain used as a reference, i.e., *Thermoanaerobacterium thermosaccharolyticum* in the present study [8,9]. On the basis of phylogenetic and physiological differences, we propose that strain mel9^T be classified as a new *Thermoanaerobacterium* species, for which the name *Thermoanaerobacterium bryantii* is suggested, in honor of the anaerobic microbiologist Marvin P. Bryant. The GenBank accession number for the 16S rRNA gene sequence of strain mel9^T is AY140670, and the bacterium has been deposited at the American Type Culture Collection (ATCC) and at the German Collection of Microorganisms and Cell Cultures (DSMZ) with the reference numbers BAA-415 and DSM 14765, respectively.

on 30 January 2022) [10] and the domain architectures are shown in Figure 3B. The two oxidoreductases were predicted to have two tightly packed domains, including a classic N-terminal Rossmann-fold NAD binding domain and a C-terminal GFO-IDH-MocA domain. The latter domain is responsible for specific binding to a particular substrate [11–13]. All of the other five putative hemicellulases only have a single domain (Figure 3B). The seven enzymes were successfully expressed in *E. coli* and purified to near homogeneity. The apparent molecular masses of the purified recombinant proteins corresponded well with the calculated values (Figure 3C). Interestingly, a similar hemicellulase gene cluster was also identified in the genomes of three members of the genus *Thermoanaerobacterium*. These bacteria are *T. xylanolyticum*, *T. thermosaccharolyticum*, and *T. saccharolyticum*. In contrast, the gene cluster was absent in the genomes of *T. italicus*, *T. mathranii*, and other known *Thermoanaerobacterium* species (Figure 3A). The amino acid sequences of the *T. bryantii* genes were aligned with those of the *T. xylanolyticum*, *T. thermosaccharolyticum*, and *T. saccharolyticum*, and the percent identities of the proteins are presented in Supplemental Table S2.

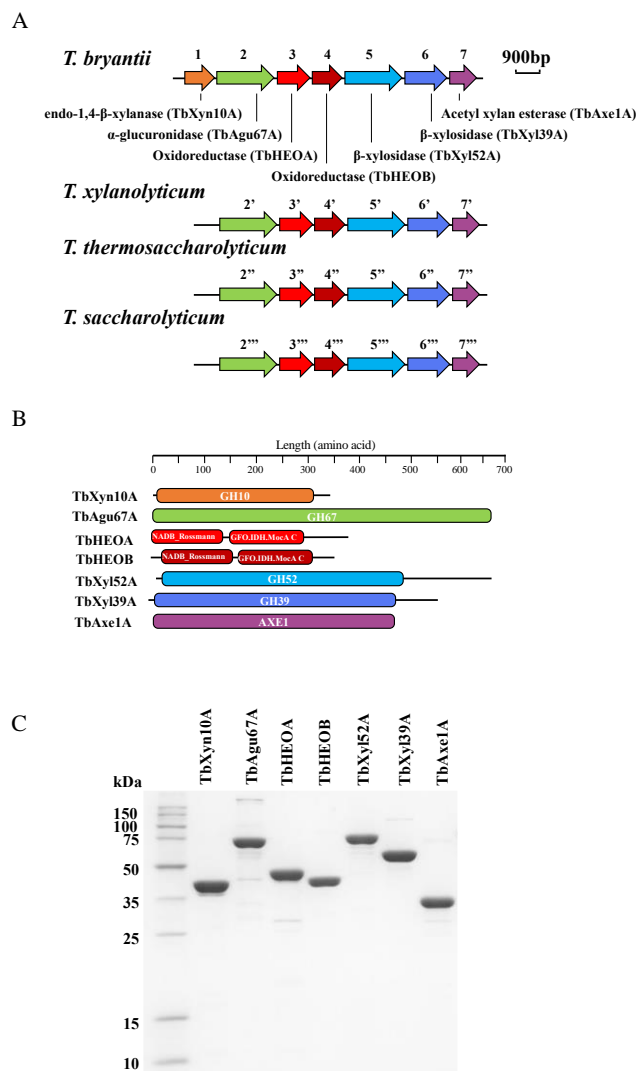


Figure 3. The *Thermoanaerobacterium bryantii* hemicellulase gene cluster. (A) The arrangement of genes in the *T. bryantii* hemicellulase gene cluster is similar but not identical to those of *T. xylanolyticum*, *T. thermosaccharolyticum*, and *T. saccharolyticum*. (B) Schematic representation of the modular architecture of the putative enzymes encoded by the *T. bryantii* hemicellulase gene cluster.

GH10: glycoside hydrolase family 10 module; GH67: glycoside hydrolase family 67 module; NADB_Rossmann: Oxidoreductase family, NAD(P)-binding Rossmann fold, which is also designated GFO-IDH-MocA in the Pfam database; GFO-IDH-MocA C: Oxidoreductase family, C-terminal alpha/beta domain (GFO is a glucose-fructose oxidoreductase, IDH is an inositol dehydrogenase, and MocA is a rhizopine catabolism protein); GH52: glycoside hydrolase family 52 module; GH39: glycoside hydrolase family 39 module; AXE1: Acetyl xylan esterase. (C) SDS-PAGE analysis of the seven enzymes encoded by the *T. bryantii* hemicellulase gene cluster. Two μg of each enzyme was resolved on a 12% SDS polyacrylamide gel.

2.4. Kinetic Parameters of TbXyn10A, TbXyl39A, TbXyl52A, and TbAxe1A

Several xylan substrates with varying complexities from different plant sources, including soluble wheat arabinoxylan (WAX), birchwood xylan (BWX), oat spelt xylan (OSX), beechwood xylan (BeeWX), and larchwood xylan (LWX), were used as substrates to estimate the kinetic parameters of the endoxylanase TbXyn10A. Thus, the soluble wheat arabinoxylan or WAX used in the present report is composed mostly of xylose chains in β -1,4 glycosidic linkages with arabinose side chains. In addition to these linkages, oat spelt xylan and birchwood xylan are reported to also contain uronic acid at 1.8% and 10.3%, respectively [14,15], while the WAX used in the present studies is likely to be devoid of uronic acids. Furthermore, xylans that are derived from hardwoods, such as birchwood xylan, are *O*-acetyl-(4-*O*-methylglucurono) xylans and contain one α -(1 \rightarrow 2)-linked 4-*O*-methylglucuronic acid substituted every 10 to 20 xylose residues [16,17]. These differences thus indicate that different combinations of xylan-targeting enzymes will be required to function synergistically to degrade the different xylans used in the present study. The TbXyn10A exhibited the highest turnover number (k_{cat}) of 853 s^{-1} and a catalytic efficiency (k_{cat}/K_m) of $184 \text{ mL mg}^{-1} \text{ s}^{-1}$ on WAX, a substrate that is less complex in its composition compared to OSX and BWX [18]. The turnover numbers on the LWX, OSX, BeeWX, and BWX were 165, 131, 88, and 36 s^{-1} , respectively. Due to a lower K_m for BWX and BeeWX, they exhibited catalytic efficiencies (k_{cat}/K_m) of 20 and $55 \text{ mL mg}^{-1} \text{ s}^{-1}$, respectively. The higher K_m values of OSX and LWX led to catalytic efficiencies of 17.7 and $23 \text{ mL mg}^{-1} \text{ s}^{-1}$ for the two xylans (Table 1).

Table 1. Kinetics parameters of TbXyn10A, TbXyl52A, TbXyl39A, and TbAxe1^a.

| Enzyme | Substrate ^b | k_{cat} (s^{-1}) | K_m (mg/mL) | k_{cat}/K_m ($\text{mL mg}^{-1} \text{ s}^{-1}$) |
|----------|--|--------------------------------------|---------------|---|
| TbXyn10A | WAX | 853 ± 84 | 4.6 ± 1.2 | 184 ± 52 |
| | OSX | 131 ± 9.4 | 7.4 ± 1.3 | 17.7 ± 3.4 |
| | BWX | 36.0 ± 0.9 | 1.8 ± 0.2 | 20.2 ± 2.1 |
| | BeeWX | 87.8 ± 3.5 | 1.6 ± 0.3 | 55.2 ± 9.0 |
| | LWX | 165 ± 9.2 | 7.1 ± 1.2 | 23.2 ± 4.0 |
| TbXyl39A | <i>p</i> NP- β -D-xylopyranoside | 20.4 ± 0.7 | 0.5 ± 0.1 | 44.7 ± 7.2 |
| TbXyl52A | <i>p</i> NP- β -D-xylopyranoside | 97.0 ± 2.5 | 0.2 ± 0.0 | 443 ± 56 |
| TbAxe1A | <i>p</i> NP-acetate | 40.8 ± 2.2 | 0.2 ± 0.1 | 171 ± 46 |

^a: The reactions were carried out at 65 °C except for TbXyl52A and TbAxe1A, which were performed at 60 and 70 °C, respectively. ^b: OSX: oat-spelt xylan; LWX: larchwood xylan; BWX: birchwood xylan; BeeWX: beechwood xylan; WAX: soluble wheat arabinoxylan.

The kinetic parameters of TbXyl39A, TbXyl52A, and TbAxe1A on *p*NP-linked substrates were also determined. The substrate for the two xylosidases, i.e., TbXyl39A and TbXyl52A, was *p*NP- β -D-xylopyranoside, and the substrate for TbAxe1A was *p*NP-acetate. TbXyl52A showed a higher catalytic efficiency ($443 \text{ mL mg}^{-1} \text{ s}^{-1}$) than TbXyl39A ($44 \text{ mL mg}^{-1} \text{ s}^{-1}$) (Table 1). TbAxe1A exhibited a k_{cat}/K_m of $171 \text{ mL mg}^{-1} \text{ s}^{-1}$ on *p*NP-acetate (Table 1).

2.5. Hydrolytic Pattern of TbXyl39A and TbXyl52A on Xylo-Oligosaccharides

TbXyl39A and TbXyl52A at a final concentration of 1 μM were incubated with xylose (X1) and xylo-oligosaccharides (X2–X6) for 20 h. Both enzymes converted xylo-oligosaccharides to xylose, based on thin-layer chromatography. The results confirmed TbXyl39A and TbXyl52A as β -xylosidases (Figure 4A). Interestingly, incubation of TbXyl39A or TbXyl52A at a lower concentration (0.1 μM) with xylotriose (X3) or xylohexaose (X6) in a time course analysis led to detection of transglycosylation activities in the two enzymes. When each of the two β -xylosidases were incubated with X3 at different time points, in addition to releasing xylose and xylobiose, larger chains, i.e., X4 to X6, were made due to the transglycosylation activity of each of the β -xylosidases (Figure 4B). The *T. bryantii* TbXyl39A appeared to have a higher transglycosylase activity than TbXyl52A (Figure 4B). In the time course analysis, TbXyl52A almost completely converted X3 and X6 to xylose after a 20 min reaction. Thus, TbXyl52A showed higher hydrolytic activity than TbXyl39A, since the latter enzyme could not completely convert X3 and X6 to xylose even after hydrolysis for 960 min (Figure 4B,C). When different concentrations (0, 5, 10, 20, 40, 60, 100 nM) of TbXyl39A or TbXyl52A were incubated with xylotriose for a short time (2 min), TbXyl39A exhibited comparable xylosidase and transglycosylase activities, and failed to produce xylose as an end product. On the other hand, TbXyl52A exhibited a higher β -xylosidase activity than transglycosylase activity at all concentrations, and converted almost all of the xylotriose present in the reaction mixture to xylose when 100 nM of enzyme was used (Figure 4D). Interestingly, when TbXyl39A was incubated with xylotriose at different temperatures (4–80 $^{\circ}\text{C}$) for 5 min, both its hydrolysis and transglycosylation activity remained nearly constant at these temperatures, except for 4 $^{\circ}\text{C}$ (Figure 4E). On the contrary, TbXyl52A behaved like a typical thermophilic enzyme, since its hydrolyzing activity was highest at 60 $^{\circ}\text{C}$ but decreased when the temperatures were either lower or higher than 60 $^{\circ}\text{C}$ (Figure 4E).

2.6. Synergistic Hydrolysis of Aldouronic Acid Mixture by TbAgu67A and the Two β -Xylosidases

Aldouronic acids were prepared by the manufacturer (Megazyme) by acid hydrolysis of glucurono-xylan, followed by chromatographic separation of the oligomers. The aldouronic acids are, therefore, different sized xylo-oligosaccharides with methyl-glucuronic acid side chains, and will require both α -glucuronidase (TbAgu67A) and β -xylosidase activities for complete hydrolysis. TbAgu67A incubated alone released xylose and xylo-oligosaccharides (X2–X4) from the aldouronic acid mixture (Figure 5). Either TbXyl39A (Figure 5A) or TbXyl52A (Figure 5B) incubated alone with substrate released xylose from the aldouronic acid mixture. When TbXyl52A and TbAgu67A were incubated together with the aldouronic acid mixture, a large amount of xylose was released (Figure 5B). Little to no xylo-oligosaccharides were detected in the reaction containing the Agu67A and the β -xylosidase. A dominant peak at 14.4 min, which represented a component of the unhydrolyzed aldouronic acid mixture, almost disappeared in the reaction with TbAgu67A. Similarly, when TbXyl39A and TbAgu67A were incubated together with the aldouronic acid mixture, a larger amount of xylose was released than during the reaction with either TbAgu67A or TbXyl39A alone. The peak at 14.4 min almost disappeared. However, when an even higher concentration (400 nM) of TbXyl39A was used than that of TbXyl52A (100 nM), a small xylobiose peak was still detected, indicating that the cleavage of xylobiose was incomplete and TbXyl39A showed a lower hydrolytic capacity than TbXyl52A. These results demonstrated that both TbXyl39A and TbXyl52A exhibited synergistic effects with TbAgu67A in hydrolyzing the aldouronic acid mixture.

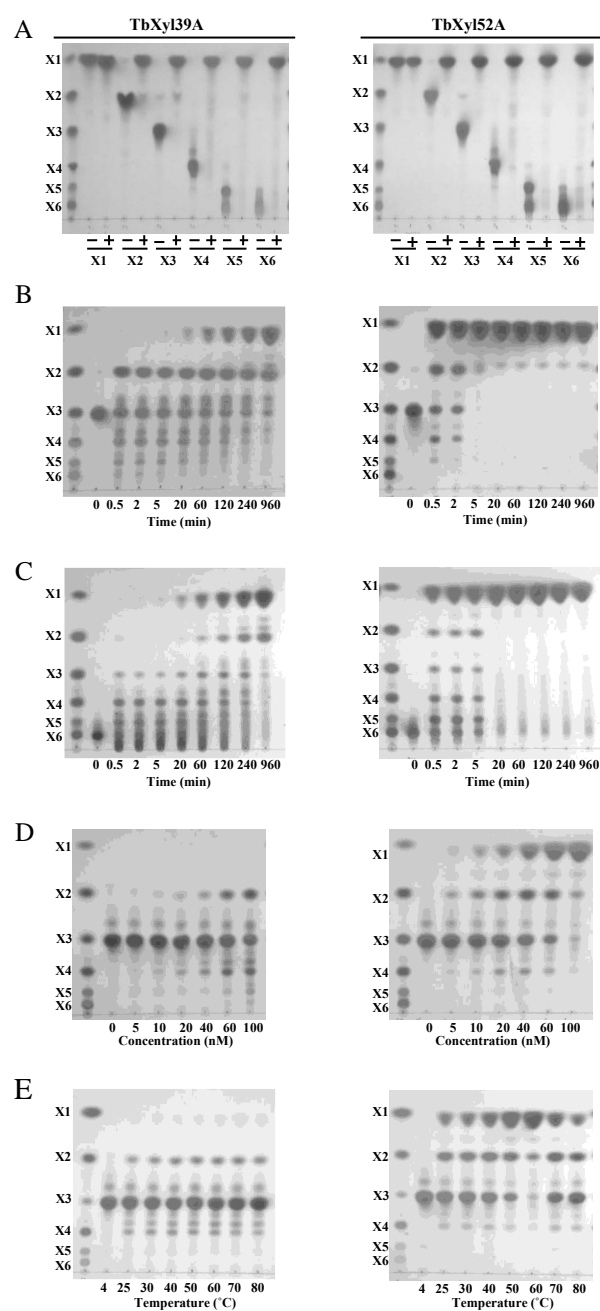


Figure 4. TbXyl39A and TbXyl52A behave differently during hydrolysis of xylo-oligosaccharides. (A) Reaction of xylose and xylo-oligosaccharides with TbXyl39A and TbXyl52A. The reactions were carried out by incubating 1 μ M of TbXyl39A or TbXyl52A with 1 mg/mL of xylose or xylo-oligosaccharides (X2–X6) at 60 $^{\circ}$ C in a citrate buffer for 20 h. (B) Hydrolysis of xylotriose by TbXyl39A or TbXyl52A. One mg/mL of xylotriose was incubated with 100 nM of TbXyl39A or TbXyl52A at 60 $^{\circ}$ C in a citrate buffer. At different time intervals (0, 0.5, 2, 5, 20 min, 1, 2, 4, and 16 h), 30 μ L samples were taken out and immediately heated at 100 $^{\circ}$ C to inactivate the enzymes. (C) Hydrolysis of xylohexaose by TbXyl39A or TbXyl52A. The experiments were carried out as described for xylotriose hydrolysis, except with xylohexaose replacing xylotriose. (D) Hydrolysis of xylotriose by TbXyl39A or TbXyl52A with increasing enzyme concentrations. One mg/mL of xylotriose was incubated with 0, 5, 10, 20, 40, 60, or 100 nM of TbXyl39A (or TbXyl52A) at 60 $^{\circ}$ C in a citrate buffer for 2 min. (E) Hydrolysis of xylotriose by TbXyl39A or TbXyl52A at different temperatures. One mg/mL of xylotriose was incubated with 100 nM of TbXyl39A (or TbXyl52A) at 4, 22, 30, 40, 50, 60, 70, or 80 $^{\circ}$ C in a citrate buffer for 5 min, respectively. All reaction products were dried and dissolved in 4 μ L of H₂O. One μ L of the end products was analyzed by thin-layer chromatography. Xylose (X1) and xylo-oligosaccharides (X2–X6) were used as standards.

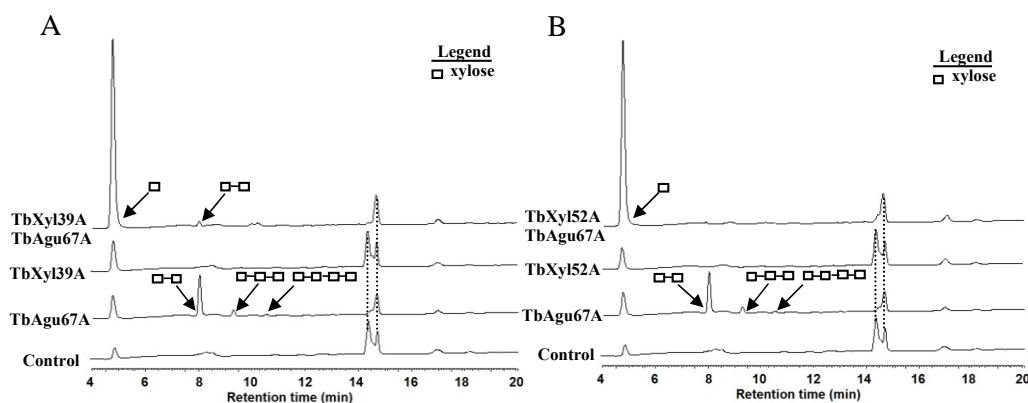


Figure 5. Synergistic effects between TbAgu67A and each of the two β -xylosidases (TbXyl39A and TbXyl52A) in hydrolysis of aldouronic acids. (A,B) HPAEC-PAD analysis of aldouronic acids incubated with TbAgu67A alone or with TbXyl39A (A) or TbXyl52A (B). 400 nM of TbXyl39A (or 100 nM of TbXyl52A) and 200 nM of TbAgu67A were incubated individually or together with 1 mg/mL of aldouronic acids in a total volume of 30 μ L, at 60 $^{\circ}$ C in the citrate buffer (pH 5.5) for 1 h. The end products of hydrolysis were diluted (400-fold) and centrifuged before analysis by HPAEC-PAD. Xylose (X1) and xylo-oligosaccharides (X2–X6) were used as standards.

2.7. The Two Oxidoreductases Improve Hydrolysis of Xylans by the *T. bryantii* Hemicellulases

TbXyn10A was the only enzyme that released significant reducing ends when the *T. bryantii* hemicellulases were individually incubated with BWX (Supplemental Figure S1A). TbXyn10A released xylobiose, xylotriose, and xylo-tetraose, as analyzed by the TLC (Supplemental Figure S1B). As mentioned above, the two xylosidases (TbXyl39A and TbXyl52A) exhibited a hydrolytic activity only by degrading xylo-oligosaccharides into xylose when the enzyme concentrations were high (Figure 4D) and the reaction times were long (Figure 4B,C). Therefore, TbXyl39A and TbXyl52A were expected to act in synergy with TbXyn10A to hydrolyze xylans. Indeed, the addition of TbXyl39A and TbXyl52A increased the released reducing sugars to 2.0 ± 0.2 mM, compared to 1.2 ± 0.1 mM by TbXyn10A alone during hydrolysis of BWX (Figure 6Ai). The addition of TbAgu67A led to a slight increase in the reducing sugars released from the xylanolytic enzymes (TbXyn10A, TbXyl39, and TbXyl52). However, the addition of TbAxe1A did not result in any significant increase in the amount of reducing sugars released. Neither of the two oxidoreductases alone showed any detectable hydrolysis of BWX in the reducing sugar assay (Supplemental Figure S1). The oxidoreductases also showed an inability to hydrolyze xylo-oligosaccharides (X2–X6) (data not shown). However, the addition of the two oxidoreductases to the mixture of TbXyn10A, TbXyl39A, and TbXyl52A improved hydrolysis of BWX. The reaction mixture with the five proteins released 5.7 mM reducing ends, which was three-fold of that produced by the three enzymes (Figure 6A). Therefore, the two oxidoreductases were named Hemicellulase-Enhancing Oxidoreductases (HEOs).

We postulated that adding metal ions and/or redox cofactors will increase the hydrolysis of the hemicelluloses by the enzymes to even higher levels, since several oxidoreductases were reported to require divalent metal ions and redox-active cofactors for maximal enhancement of biomass deconstruction [3–7,19,20]. Therefore, three different divalent metal ions (Mn^{2+} , Mg^{2+} , or Zn^{2+}) were individually added to the five-enzyme mixture (i.e., TbXyn10A, TbXyl39A, TbXyl52A, TbHEOA, and TbHEOB) to evaluate their effects on BWX depolymerization. Only Mn^{2+} enhanced the hydrolysis of BWX by the five enzymes (5Es) in the reducing sugar assay (Figure 6Bi), and its addition slightly increased the amount of xylose released by the 5Es in the TLC analysis (Figure 6Bii).

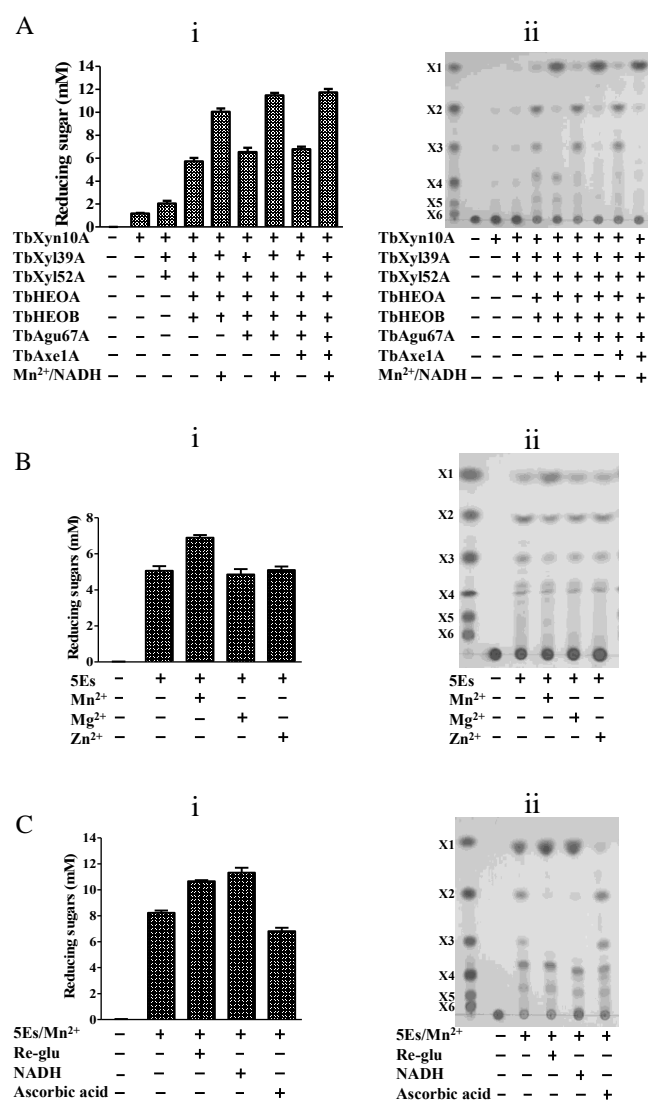


Figure 6. Effect of different divalent metal ions and redox-active cofactors on the hemicellulase-enhancing activities of two oxidoreductase-like polypeptides, TbHEOA and TbHEOB, during hydrolysis of BWX by hemicellulases (TbXyn10A, TbXyl39A, TbXyl52A, TbAgu67A, and TbAxe1A). (A) Analysis of the effect of different divalent metal ions on hydrolysis of BWX by 5Es (TbXyn10A, TbXyl39A, TbXyl52A, TbHEOA, and TbHEOB). Five mg/mL of BWX was incubated with the five-enzyme mixture (10 nM TbXyn10A, 10 nM TbXyl39A, 5 nM TbXyl52A, 50 nM TbHEOA, and 50 nM TbHEOB) at 60 °C in a citrate buffer (pH 5.5) for 16 h, in the absence or presence of different metal ions (1.0 mM Mn²⁺, 1.0 mM Mg²⁺, or 1.0 mM Zn²⁺, respectively). (B) Analysis of the effect of different redox-active cofactors on hydrolysis of BWX by 5Es. The experiment was carried out by incubating 5 mg/mL of BWX with the five enzymes mixture (10 nM TbXyn10A, 10 nM TbXyl39A, 5 nM TbXyl52A, 100 nM TbHEOA, and 100 nM TbHEOB) at 60 °C in a citrate buffer (pH 5.5) with 1 mM Mn²⁺ for 16 h in the absence or presence of different cofactors (1 mM NADH, 1 mM Ascorbic acid, and 0.5 mM Re-glu, respectively). (C) Analysis of the effect of Mn²⁺ and NADH on hydrolysis of BWX by different combinations of the seven enzymes (TbXyn10A, TbXyl39A, TbXyl52A, TbHEOA, TbHEOB, TbAgu67A, and TbAxe1A) encoded in the *T. bryantii* hemicellulase gene cluster. Five mg/mL of BWX was incubated with different combinations of the seven enzymes (10 nM TbXyn10A, 10 nM TbXyl39A, 5 nM TbXyl52A, 100 nM TbAgu67A, 100 nM TbAxe1A, 100 nM TbHEOA, and 100 nM TbHEOB) at 60 °C in a citrate buffer (pH 5.5) for 16 h, in the presence or absence of 1 mM of NADH and 1 mM of MnSO₄. The end products of hydrolysis were analyzed through the reducing sugar assay (i) and TLC (ii). 5Es is defined as the five-enzyme mixture (TbXyn10A, TbXyl39A, TbXyl52A, TbHEOA, and TbHEOB). Other abbreviations were, X1: xylose; X2: xylobiose; X3: xylotriose; X4: xylotetraose; X5: xylopentaose; X6: xylohexaose; Re-glu: reduced glutathione.

Both TbHEOA and TbHEOB were predicted to have a NAD-binding domain. Since redox-active cofactors were suggested to play an important role in the oxidoreductase activity in some reports [7,19,20], three reductants (NADH, ascorbic acid, and reduced glutathione (Re-glu)) were tested for their capacity to enhance the activities of TbHEOA and TbHEOB. In the presence of Mn^{2+} , either NADH or Re-glu, but not ascorbic acid, could increase the hydrolytic activity of the five enzymes on BWX in the reducing sugar assay (Figure 6Ci). A TLC analysis clearly showed that much less xylobiose and xylotriose were produced when NADH and Re-glu were included in the reaction than in the absence of the cofactors (Figure 6Cii). The addition of ascorbic acid decreased the hydrolytic activity of the five enzymes on BWX (Figure 6Ci). Furthermore, the TLC analysis demonstrated that xylose release was less in the presence of ascorbic acid than in the reaction without cofactors (Figure 6Ci). In the absence of Mn^{2+} , Re-glu alone could not increase the hydrolyzing efficiency of the five enzymes (Supplemental Figure S2). In the presence of Mn^{2+} and NADH, the addition of Re-glu did not result in a further improvement (Supplemental Figure S2). It should be noted that in the absence of TbHEOA and TbHEOB, Mn^{2+} and NADH did not show any obvious improvements on the hydrolytic activity of the three enzymes on BWX (data not shown). Therefore, Mn^{2+} and NADH acted as cofactors of TbHEOA and TbHEOB, but not of the three enzymes (TbXyn10A, TbXyl39A, and TbXyl52A). The addition of Mn^{2+} and NADH to the five enzymes released more reducing ends (10.0 ± 0.3 mM) than incubation with only the five enzymes alone (5.7 ± 0.3 mM) (Figure 6Ci). Therefore, in the presence of the co-factors, the xylanolytic activity of the five-enzyme mixture was almost doubled.

The enhancing role of the cofactors in enzymatic activity was not limited to the combination of the five-enzyme mixture (5Es). The addition of Mn^{2+} and NADH could also improve the hydrolyzing efficiency of a six-enzyme mixture (6Es, including TbXyn10A, TbXyl39A, TbXyl52A, TbHEOA, TbHEOB, and TbAgu67A) and a seven-enzyme mixture (7Es, including TbXyn10A, TbXyl39A, TbXyl52A, TbHEOA, TbHEOB, TbAgu67A, and TbAxe1A) on BWX by increasing the release of reducing ends, from 6.5 ± 0.4 to 11.5 ± 0.2 mM (for 6Es) and from 6.8 ± 0.2 to 11.7 ± 0.3 mM (for 7Es), respectively (Figure 6Ai). The TLC analysis clearly showed that much less xylobiose and xylotriose were produced when NADH and Mn^{2+} were added to the reaction of 6Es or 7Es than that when no cofactor was added, as was also observed for the 5Es experiments (Figure 6Aii).

2.8. Hydrolysis of Xylan by the Seven Enzymes Encoded by the Hemicellulase Gene Cluster

Xylans may be different in their composition and complexity depending on their plant source. Therefore, five xylans (WAX, BWX, OSX, BeeWX, and LWX) [15,18,21,22], as well as a more complex plant substrate, Miscanthus, with intact cellulose, hemicellulose, and lignin [23,24], were tested for synergistic activities of the seven *T. bryantii* enzymes. The results in Figure 7 demonstrate that synergistic effects existed in the hydrolysis of xylans by the 7Es. However, the degrees of synergy were different, most likely due to the composition/structure of the xylan substrates. TbXyn10A released moderate amounts of reducing sugars from all xylans tested (Lane 1 in Figure 7), and xylo-oligosaccharides (X1, X2, and X3) were the end products (Supplemental Table S3). The addition of the two β -xylosidases (TbXyl39A and TbXyl52A) and the two HEOs (TbHEOA and TbHEOB) improved the deconstruction of BWX, BeeWX, OSX, LWX, and Miscanthus, releasing increasingly reducing ends when they were added successively (Lane 2–Lane 7 in Figure 7A–D,F), with larger amounts of xylose as their end products (Supplemental Table S3). WAX has the simplest composition in the xylans tested, and the increase in the release of reducing ends from this substrate was the lowest among all xylans tested (Lane 2–Lane 7 in Figure 7E). Indeed, the released end products (mainly X1 and X2) only increased slightly by successive addition of the four enzymes to TbXyn10A in the hydrolysis of WAX (Supplemental Table S3). TbAgu67A and TbAxe1 greatly changed the hydrolysis of complex xylan substrates by the 5Es (TbXyn10A, TbXyl39A, TbXyl52A, TbHEOA, and TbHEOB). On BWX, either TbAgu67A or TbAxe1A, or their combination, could enhance the hydrolytic efficiency of the 5Es, releasing more

reducing ends (Lane 8–Lane 10 in Figure 7B). On OSX, the addition of TbAgu67A, TbAxe1A, or their combination, slightly increased the hydrolytic activity of the 5Es compared to that of the 5Es without these accessory enzymes (Lane 8–Lane 10 in Figure 7C). On BeeWX and LWX, TbAgu67A increased the release of reducing ends when it was added to the 5Es (Lane 8 in Figure 7A,D). However, the addition of TbAxe1 did not improve the hydrolysis of either BeeWX or LWX (Lane 9 and Lane 10 in Figure 7A,D). On WAX and Miscanthus, the addition of each of the two β -xylosidases (TbXyl139A and TbXyl152A) led to an increase in the reducing sugars released (Lane 2–Lane 3 Figure 7E,F). However, neither TbAgu67A nor TbAxe1 could notably improve the hydrolysis (Lane 8–Lane 10 in Figure 7E,F) in the reducing sugars assay. Except for WAX, the HPLC quantification of the end products, in general, showed a clearer improvement of end-product release upon addition of TbAgu67A or TbAxe1A individually or in combination in the hydrolysis of the different xylans (Supplemental Table S3).

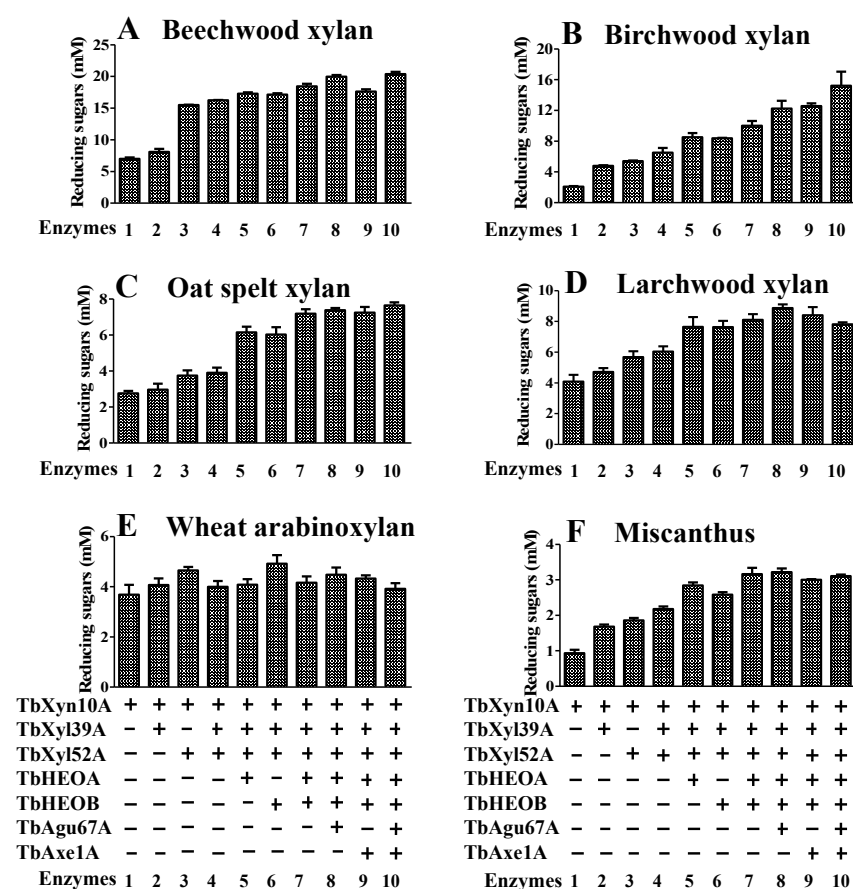


Figure 7. The synergistic effect of the seven enzymes encoded in the *T. bryantii* hemicellulase gene cluster during hydrolysis of heterogeneous xylans (A–E) and Miscanthus (F). The enzymatic reactions were carried out at 60 °C in a pH 5.5 citrate buffer supplemented with 1.0 mM of NADH and 1.0 mM of Mn²⁺. Substrates (BeeWX, BWX, LWX, and OSX) at 5 mg/mL were incubated with different combinations of the seven enzymes (10 nM TbXyn10A, 10 nM TbXyl139A, 5 nM TbXyl152A, 100 nM TbAgu67A, 100 nM TbAxe1A, 50 nM TbHEOA, and 50 nM TbHEOB) for 16 h. In the case of WAX, a lower concentration of substrate (2.5 mg/mL) was incubated with a lower concentration of enzymes (5 nM TbXyn10A, 5 nM TbXyl139A, 2.5 nM TbXyl152A, 50 nM TbAgu67A, 50 nM TbAxe1A, 25 nM TbHEOA, and 25 nM TbHEOB) for 16 h. Miscanthus was incubated at a higher substrate loading (10 mg/mL of Miscanthus) with higher concentrations of enzymes (1 μ M TbXyn10A, 0.5 μ M TbXyl139A, 0.5 μ M TbXyl152A, 2 μ M TbHEOA, 2 μ M TbHEOB, 2 μ M TbAgu67A, and 2 μ M TbAxe1A) for a longer period of 21 h. The released reducing sugars were determined using the pHBAH method.

3. Discussion

T. bryantii was isolated for its potential utility in the production of thermostable α -galactosidase, an enzyme for application in the food industry. The genus *Thermoanaerobacterium* is, however, known to be endowed with plant cell wall-degrading enzymes that can be harnessed for enzymatic release of fermentable sugars from plant cell wall polysaccharides, such as cellulose and hemicellulose. Enzymatic deconstruction of plant cell wall polysaccharides is a critical step in the production of second-generation biofuels from biomass. For this reason, the genome of *T. bryantii* was partially sequenced to search the genome for plant cell wall-degrading enzymes. In this study, seven enzymes encoded in a *T. bryantii* putative hemicellulase gene cluster were expressed, and the proteins were purified and biochemically characterized. All enzymes were thermophilic and exhibited optimal temperatures in a range of 60 to 70 °C. The amino acid sequence of TbXyn10A was used in searching the NCBI GenBank non-redundant protein database. Interestingly, most of the TbXyn10A homologs with an amino acid sequence identity above 47% to TbXyn10A also lacked the predictable N-terminal signal peptide. Therefore, the data suggest that these proteins are intracellularly located [25–30]; however, it is unlikely that, at least, the endoxylanase TbXyn10A will be intracellularly located, since it will be required to degrade the complex polysaccharide extracellularly for transport of the products into the cell. The XynA of *Caldicellulosiruptor saccharolyticus* exhibited the highest identity (61%) to TbXyn10A [31], and this enzyme was reported as having an atypical signal peptide that contained charged and polar amino acids [32]. For such xylanases without a prototypical signal peptide, it has been suggested that they constitute a new type of xylanases with specific enzymatic activities in the degradation of xylan [33]. Thus, TbXyn10A and its homologs may be intracellular enzymes or cell surface enzymes that hydrolyze short xylo-oligosaccharides. Nevertheless, these enzymes may also be extracellular enzymes exported via a non-canonical secretion pathway [33,34]. In spite of the uncertainty in its location after expression, TbXyn10A functioned as the main endoxylanase in the *T. bryantii* hemicellulase xylanolytic gene cluster. The enzyme depolymerized the xylan backbone in simple and complex xylans into xylo-oligosaccharides and their derivatives (Supplemental Figure S1 and Table S3).

Endoxylanases hydrolyze the xylan backbone into xylo-oligosaccharides, which are then further converted by β -xylosidases into xylose. Two β -xylosidases (TbXyl39A and TbXyl52A) are encoded in the *T. bryantii* hemicellulase gene cluster. The two enzymes were different from each other in their biochemical characteristics, and therefore they can be considered functionally non-redundant, as observed in our earlier report [35]. TbXyl52A had a much higher catalytic efficiency (k_{cat}/K_m) on *p*NP- β -D-xylopyranoside (~10-fold) than TbXyl39A (Table 1). While the hydrolytic activity of TbXyl52A was sensitive to temperature, the enzymatic activity of TbXyl39A on the same substrate was not discernibly affected over a wide range of temperature. In addition, TbXyl52A appeared to hydrolyze xylo-oligosaccharide more efficiently than TbXyl39A, in agreement with their estimated catalytic efficiencies on the artificial substrate, *p*NP- β -D-xylopyranoside. When the enzyme concentrations were low, both TbXyl39A and TbXyl52A had transglycosylase activities in the initial stage of xylo-oligosaccharide hydrolysis. Members in both the GH39 and GH52 family display a retaining reaction mechanism [36,37], which involves the formation of a glycosyl–enzyme intermediate. This intermediate can be decomposed either by the action of a nucleophilic water molecule leading to hydrolysis, or an attack by some other suitable nucleophile leading to transglycosylation [38]. This mechanism likely explains the hydrolysis and transglycosylase activities possessed by TbXyl39A and TbXyl52A. In contrast, when the enzyme concentrations were raised and the incubation times were extended, only xylose or short oligosaccharides were identified in the end products of the reaction, especially for TbXyl52A. These analyses are critical for the application of these enzymes in industrial processes. High loading or optimization of enzymes will be required in these processes to prevent transglycosylation, an undesirable reaction in plant cell wall hydrolysis for fermentation. Considering that enzyme loading for the biofuel industry is

often high, this may be important since the transglycosylation activity is not desirable in the decomposition of hemicellulose into simple sugars.

Heterogeneous xylans are commonly substituted with acetyl, arabinofuranosyl, or 4-*O*-methyl glucuronyl groups as side chains. Therefore, accessory hemicellulases that cleave the side chains are required for complete degradation of xylan. The *T. bryantii* hemicellulase gene cluster encodes two such accessory enzymes, i.e., TbAgu67A and TbAxe1A. The two enzymes exhibited similar optimal pH and temperatures to TbXyn10A, TbXyl39A, and TbXyl52A, which facilitates the reconstitution of a thermophilic hemicellulase mixture. As expected, the addition of the two accessory enzymes vastly improved the hydrolysis of xylan by the *T. bryantii* endoxylanase and β -xylosidases.

Each of the two HEOs (TbHEOA and TbHEOB) possesses an N-terminal Rossmann α/β -fold NAD-binding domain and a C-terminal GFO-IDH-MocA domain, and this further confirms their identification as members of the oxidoreductase family. The N-terminal NAD-binding domain is responsible for the binding of NAD(P)H/NAD(P)⁽⁺⁾, and the C-terminal GFO-IDH-MocA domain, consisting of several antiparallel β -strands, is responsible for the binding of a specific substrate to catalyze a particular enzymatic reaction. The members in the GFO/IDH/MocA family utilize NAD(H) or NADP(H) as the cofactor, and have been shown to possess diverse functions [12,13,39–41]. The oxidoreductase from *Caulobacter crescentus* CB15 that belongs to the GFO/IDH/MocA protein family has been shown to convert D-xylose to both its oxidized (xylonate) and reduced form (xylitol) [42]. The classical oxidoreductase of GFO from *Zymomonas mobilis* is a glucose-fructose oxidoreductase, which oxidizes D-glucose to D-gluconolactone with NADP, and then reduces D-fructose into D-sorbitol with NADPH, with a single site for four substrates, including glucose, fructose, gluconolactone, and sorbitol [43]. All of the characterized members of this family showed very low identities to TbHEOA and TbHEOB, and the two HEOs of *T. bryantii* also shared very low amino acid sequence identity (15%). Only the motif of Glu-Lys-Pro (EKP) in the Rossmann fold, which is supposed to have a pivotal role in the function of the protein [11], is conserved in TbHEOA. In TbHEOB, a conservative change has led to Asp-Lys-Pro (DKP) as the conserved motif (Supplemental Figure S4). Therefore, TbHEOA and TbHEOB likely carry out similar oxidoreductive reactions utilizing NAD(H). Experimentally, TbHEOA and TbHEOB did not have any discernible activity on xylan, xylose, and xylo-oligosaccharides (X2–X6) in both the reducing sugar assay and TLC analysis. In contrast, the addition of TbHEOA and TbHEOB significantly enhanced degradation of the heterogeneous xylans by enzyme mixtures containing three or five hemicellulases in the present report. The enhancing effect was more significant when a metal ion, Mn²⁺, and the cofactor NADH were added to the reaction mixture. The mechanism by which TbHEOA and TbHEOB enhanced hydrolysis of xylan by the *T. bryantii* hemicellulases is still under investigation. However, there seemed to be some clues in our results. The presence of either TbHEOA or TbHEOB or their combination generated two unidentified products, which appeared as the spots between X3 and X4 and between X4 and X5 on the TLC plate when BWX was hydrolyzed by the 3Es (Supplemental Figure S3B). These products were significantly diminished when TbAgu67A was added to the reaction (Supplemental Figure S3A,B,F). Therefore, TbHEOA and TbHEOB might act on some intermediate products in xylan hydrolysis.

The gene structure of the two tandemly arranged oxidoreductases (TbHEOA and TbHEOB) from *T. bryantii* is conserved in other bacteria (Supplemental Table S4). Among the two tandemly arranged oxidoreductases, homologs of TbHEOA all have the conserved motif (EKP), whereas homologs of TbHEOB have 'DKP' and 'DKA' as the conserved motif (Supplemental Figure S5). Many of the bacteria harboring homologs of the two HEOs decompose xylan or other plant biomass [44–51]. For the rest of the bacteria, most are of *Enterobacter* species (Supplemental Table S4). Some species of *Enterobacter* were also reported to efficiently degrade plant cellulosic biomass [52–54]. Thus, we hypothesized that homologs of the two HEOs play a pivotal role in the deconstruction of biomass by these strains.

In addition to TbHEOA and TbHEOB, there are several enzymes which are not canonical glycoside hydrolases, but their presence could also dramatically increase the breakdown of plant polysaccharides by glycoside hydrolases. Such proteins include CBP21 from *Serratia marcescens* (previously classified as a CBM33 protein) [19], CelS2 from *Streptomyces coelicolor* A3-(2) [20], which is composed of a CBM33 domain and a C-terminal CBM2 domain, and the formerly well-known enigmatic fungal GH61 endoglucanases [3–7]. These proteins have weak hydrolytic activity on recalcitrant polysaccharides, such as chitin and crystalline cellulose. However, they can dramatically increase the efficiency of chitin or cellulose hydrolysis by chitinase and cellulases, respectively, via an oxidative degradation process in which a reducing-end aldonic acid group was generated [7,19,20]. These identified facilitators of plant cell wall hydrolysis also need metal ions such as Mg^{2+} , Zn^{2+} , and Cu^{2+} , and redox-active agents for maximal activity. The GH61 proteins have already been classified into a novel enzyme family known as Polysaccharide MonoOxygenases (PMOs) [4]. Similarly, TbHEOA and TbHEOB could dramatically stimulate xylan hydrolysis by hemicellulases, and Mn^{2+} and NADH seemed to be specifically required for the observed effect of the two HEOs. The two HEOs described in the present study have low amino acid sequence identities to that of GH61 or the CBM33 proteins. Therefore, whether the two enzymes use a similar oxidative hydrolysis mechanism as that described for the GH61 or CBM33 enzymes is unknown. We look forward to experimental evidence that clearly explains the mechanism by which these two enzymes enhance plant cell wall hydrolysis by hemicellulases.

4. Materials and Methods

4.1. Materials

T. bryantii strain mel9^T was isolated from the waste pile of a canning factory in Hoopeston, Illinois, USA. The strain was classified into the *Thermoanaerobacterium* genus based on physiological, morphological, and phylogenetic studies (see below for details). The *Escherichia coli* XL10-Gold strain (Stratagene, La Jolla, CA, USA) was used for gene cloning and plasmid maintenance throughout the study, and the *E. coli* BL21-CodonPlus (DE3) RIPL strain (Stratagene, La Jolla, CA, USA) was used for protein expression. The pET-46 Ek/LIC vector (Novagen, San Diego, CA, USA) was used for gene cloning. The *p*-nitrophenyl acetate (*p*NP-acetate) was from Acros Organics (Morris Plains, NJ, USA). Isopropyl β -D-1-thiogalactopyranoside (IPTG) was purchased from Gold Biotechnology (St. Louis, MO, USA). The aldouronic acid mixture, wheat arabinoxylan (WAX, medium viscosity), and xylo-oligosaccharides were obtained from Megazyme (Wicklow, Ireland). The oat spelt xylan (OSX), beechwood xylan (BeeWX), birchwood xylan (BWX), larchwood xylan (LWX), *p*-nitrophenyl β -D-xylopyranoside (*p*NPX), L-glutathione reduced (Glu-Re), orcinol, and β -Nicotinamide adenine dinucleotide (reduced disodium salt hydrate, NADH) were purchased from Sigma-Aldrich (St. Louis, MO, USA). The PrimeSTAR HS DNA Polymerase was from Takara (Shiga, Japan). The QIAprep SpinMiniprep Kit was obtained from Qiagen (Valencia, CA, USA). The Talon metal affinity resin was purchased from Clontech Laboratories, Inc. (Mountain View, CA, USA). The Amicon[®] Ultra centrifugal filters were obtained from Millipore (Billerica, MA, USA). All other reagents and common supplies were purchased from Fisher Scientific (Pittsburgh, PA, USA).

4.2. Characterization of *T. bryantii* mel9^T

T. bryantii strain mel9^T was isolated in a minimal medium with raffinose as the sole carbon and energy source. The methods and the contents of the medium for isolating the bacterium were described in our previous report [55]. Aliquots of liquid samples from a waste pile from a corn-canning factory (Hoopeston, IL, USA) were inoculated into the minimal medium [55]. A single colony from the enrichment plate with raffinose as the sole carbon and energy source yielded several colonies with similar morphology. A single colony was picked and streaked several times to ensure the purity of the isolated colony. Further analyses yielded a bacterium that was named *T. bryantii* strain mel9^T. The

optimum, upper, and lower growth temperature limits of strain mel9^T were determined by incubation between 37 and 75 °C in the minimal medium supplemented with glucose. The isolate was grown between pH 5.0 and 8.0 at 65 °C in the same medium to determine the optimum pH for growth. The reduction of thiosulfate, sulfate, and sulfur, each at a 20 mM concentration, was tested, and microscopic examination was used to check for sulfur formation [55]. Transmission electron microscopy (TEM) and negative staining were used to examine cell morphology, as described previously [55]. Fermentation end products were analyzed by gas chromatography and high-performance liquid chromatography, as described elsewhere [55]. The 16S rRNA gene sequence of strain mel9^T was used to search the database at the GenBank and thirteen 16S rRNA gene sequences of closely related organisms were retrieved for phylogenetic analysis. The G + C content of the genomic DNA was determined by DSMZ (Deutsche Sammlung von Mikroorganismen und Zellkulturen GmbH, Braunschweig, Germany) using a chromatographic method [56]. The DNA–DNA hybridization was also performed by DSMZ using a method described earlier [57].

4.3. Genome Sequencing

The genomic DNA of *T. bryantii* was extracted as described previously [58]. The genome sequence of *T. bryantii* mel9^T was partially sequenced (W. M. Keck Center for Comparative and Functional Genomics at the University of Illinois at Urbana-Champaign) using standard procedures. Briefly, the genomic DNA sequence data were generated with one-half plate of shotgun 454 GS-FLX data and one-half plate of 8 kb paired-end GS FLX Titanium data using the 454 Life Sciences Genome Sequencer (Branford, CT, USA). The partial genome sequence was assembled by Newbler version 2.0 into 7 scaffolds comprised of 71 contigs. The genome sequence was uploaded and analyzed on the Rapid Annotation using Subsystem Technology (RAST) server (<http://rast.nmpdr.org/>) [59].

4.4. Gene Cloning, Gene Expression, and Protein Purification

The genes in this study were amplified by the PrimeSTAR HS DNA Polymerase using genomic DNA as a template (see Supplemental Table S5 for primer information). The PCR products were gel-purified using the Qiagen QIAquick Gel Extraction Kit. The resulting amplicons were then subjected to the exonuclease activity of T4 DNA polymerase to generate sticky ends. The treated DNA was annealed to the pET-46 Ek/LIC vector, and the annealed products were transformed into *E. coli* XL10-Gold competent cells. The transformants were selected on a Lysogeny broth (LB) agar plate supplemented with 100 µg/mL of ampicillin. Single colonies were picked and inoculated into 3 mL of LB medium supplemented with 100 µg/mL of ampicillin and cultured overnight. Plasmids were extracted from the cultures using the QIAprep Spin Miniprep Kit, and the inserts were verified by DNA sequencing (W. M. Keck Center for Comparative and Functional Genomics at the University of Illinois). The recombinant plasmids with the correct inserts were then transformed individually into *E. coli* BL21-CodonPlus (DE3) RIPL cells and selected on LB agar plates containing 100 µg/mL of ampicillin and 50 µg/mL of chloramphenicol at 37 °C. After overnight incubation, single colonies were inoculated into 10 mL of LB supplemented with the same antibiotics and bacterial culturing continued at 37 °C at a speed of 250 rpm for 6 h. The pre-culture was inoculated into 1 L of LB medium supplemented with the same antibiotics, and the culture was shaken at a speed of 250 rpm at 37 °C until the OD₆₀₀ (optical density at 600 nm) reached 0.3. The temperature was then shifted to 16 °C, and IPTG was added at a final concentration of 0.1 mM. Following an additional 16 h of culturing at 16 °C, the cells were harvested by centrifugation. The cell pellets were then resuspended in 40 mL of lysis buffer (50 mM Tris-HCl, 300 mM NaCl, pH 7.5) and ruptured by two passages through an EmulsiFlex C-3 cell homogenizer from Avestin (Ottawa, Canada). Since proteins encoded by *T. bryantii* were expected to be thermostable, the cell lysate was consecutively treated at 55 and 60 °C for 15 min, and the precipitated host (*E. coli*) proteins were pelleted by centrifugation at 12,857 × g for 20 min at 4 °C. The recombinant proteins in the heat-treated supernatants were purified using the Talon metal affinity chromatography

resin according to the manufacturer's instructions (Clontech, Mountain View, CA, USA). The eluted protein fractions were analyzed by sodium dodecyl sulfate-polyacrylamide gel electrophoresis (SDS-PAGE) according to Laemmli's method [60]. Eluted fractions with purified proteins were pooled, the proteins were concentrated, and the buffer was changed to a protein storage buffer (50 mM Tris-HCl, 150 mM NaCl, pH 7.5) with Amicon Ultra-15 centrifugal concentrators. The protein concentrations were measured using a NanoDrop 1000 (Thermo Fisher Scientific Inc., Waltham, MA, USA) and the Beer–Lambert law with the following extinction coefficients: 67,840, 128,160, 59,610, 50,435, 125,055, 99,490, and 35,942 $\text{M}^{-1} \text{cm}^{-1}$ for TbXyn10A, TbAgu67A, TbHEOA, TbHEOB, TbXyl52A, TbXyl39A, and TbAxe1A, respectively.

4.5. Determination of Optimal pH and Temperature

Two types of buffers were used to determine the optimal pH of TbXyn10A, TbXyl39A, TbXyl52A, and TbAxe1A: 50 mM sodium citrate—150 mM NaCl (pH 4.0 to 6.0) and 50 mM Na_2HPO_4 — NaH_2PO_4 —150 mM NaCl (pH 6.0 to 8.0). The optimal pH of TbXyn10A was determined by incubating 40 nM of TbXyn10A with 1 mg/mL of wheat arabinoxylan (WAX) at different pH values at 60 °C for 10 min. The reducing sugars released were measured using the *para*-hydroxybenzoic acid hydrazide (*p*HBAH, Sigma-Aldrich, St. Louis, MO, USA) assay [61], with xylose (Sigma-Aldrich, St. Louis, MO, USA) as the standard. Meanwhile, the optimal pH of TbXyl39A, TbXyl52A, and TbAxe1A was performed using a Cary 300 UV-visible-spectrum spectrophotometer equipped with a Peltier temperature control unit (Varian Inc., Palo Alto, CA, USA) [62], and experiments were carried out at different pH at 60 °C by incubating 10 nM of TbXyl39A (or 5 nM of TbXyl52A) with 1 mM of *p*NPX, or by incubating 80 nM of TbAxe1A with 1 mM of *p*NP-acetate, respectively. Hydrolysis of the *p*NP substrates was monitored continuously by recording the UV signal at 400 nm, and the rate of *p*NP release was determined according to standard curves of *p*NP in different pH solutions. To determine the optimal temperature, incubation of 40 nM of TbXyn10A and 1 mg/mL of WAX, 10 nM of TbXyl39A and 1 mM of *p*NPX, 5 nM of TbXyl52A and 1 mM of *p*NPX, and 80 nM of TbAxe1A and 1 mM of *p*NP-acetate were performed at their optimal pH at different temperatures, ranging from 30 to 90 °C, at 5 °C intervals, respectively.

4.6. Kinetic Studies of TbXyn10A, TbXyl39A, TbXyl52A, and TbAxe1A

The kinetic parameters of TbXyn10A were estimated at its optimal pH and temperature. The kinetic analysis of TbXyn10A with BWX, OSX, BeeWX, LWX, and WAX was performed by incubating an appropriate concentration of TbXyn10A with a range of xylan substrates at pH 5.5 and a temperature of 65 °C for 15 min. The concentration of TbXyn10A was determined by performing initial experiments with multiple time points and different enzyme concentrations to identify an enzyme concentration that yielded a linear rate over 15 min. The reducing ends released were measured using the *p*HBAH assay [61]. The velocities were plotted against the substrate concentrations, and kinetic parameters were estimated by fitting the data to a Michaelis–Menten equation using a non-linear regression model (Graphpad Prism v5.01 software, San Diego, CA, USA).

The kinetic parameters of TbXyl39A and TbXyl52A were estimated at their optimal pH and optimal temperatures with *p*NP substrates. The kinetic studies of TbXyl39A, TbXyl52A, and TbAxe1A were performed using the Cary 300 UV-visible-spectrum spectrophotometer. TbXyl39A (10 nM) was incubated with different concentrations (0–10 mM) of *p*NP- β -D-xylopyranoside (*p*NPX) in a pH 6.0 citrate buffer (50 mM of sodium citrate, 150 mM of NaCl) at 65 °C. Similarly, TbXyl52A (5 nM) was incubated with 0–8 mM of *p*NPX in a pH 5.5 citrate buffer at 60 °C, and TbAxe1A (5 nM) was incubated with 0–8 mM of *p*NP-acetate in a pH 6.5 phosphate buffer (50 mM of sodium phosphate, 150 mM of NaCl) at 70 °C. The reaction velocities were plotted against the substrate concentrations, and kinetic parameters were calculated as described above.

4.7. Reaction Patterns of TbXyl39A and TbXyl52A on Xylose and Xylo-Oligosaccharides

Reactions of TbXyl39A or TbXyl52A with xylose and xylo-oligosaccharides (xylobiose, X2; xylotriase, X3; xylo-tetraose, X4; xylopentaose, X5; xylohexaose, X6) were examined by incubating 1 μ M of Xyl39A or Xyl52A with 1 mg/mL of xylose or xylo-oligosaccharides (X2–X6) in a total volume of 40 μ L at 60 °C in a citrate buffer (pH 6.0 for Xyl39A and pH 5.5 for Xyl52A) for 20 h. One mg/mL of xylotriase or xylohexaose was incubated with 100 nM of Xyl39A or Xyl52A at 60 °C in the citrate buffer (pH 6.0 for Xyl39A and pH 5.5 for Xyl52A) in a total volume of 400 μ L, respectively, to determine the reaction patterns of Xyl39A or Xyl52A with long and short xylo-oligosaccharides. At different time intervals (0, 0.5, 2, 5, 20 min, 1, 2, 4, and 16 h), 30 μ L of sample was removed. The difference in hydrolysis of xylotriase by Xyl39A or Xyl52A was further analyzed by incubating 1 mg/mL of xylotriase with a range (0–100 nM) of Xyl39A or Xyl52A at 60 °C in a citrate buffer (pH 6.0 for Xyl39A and pH 5.5 for Xyl52A) in a total volume of 40 μ L for 2 min, or by incubating 1 mg/mL of xylotriase with 100 nM of Xyl39A or Xyl52A at 4, 22, 30, 40, 50, 60, 70, and 80 °C in the citrate buffer (pH 6.0 for Xyl39A and pH 5.5 for Xyl52A) in a total volume of 40 μ L for 5 min, respectively. The reaction products (30 or 40 μ L) were all dried using a Savant DNA 120 SpeedVac concentrator (Savant, Ramsey, MN, USA) and dissolved in 4 μ L of H₂O. Then, 1 μ L each of the end products was spotted onto thin-layer chromatography (TLC) plates with xylose and xylo-oligosaccharides (X2–X6) as standards and developed in a *n*-butanol-acetic acid-H₂O (10:5:1, vol/vol/vol) mobile phase. The sugars were then visualized by spraying with a 1:1 (vol/vol) mixture of methanolic orcinol (0.2% wt/vol) and sulfuric acid (20% vol/vol), followed by heating at 100 °C for 5 min, as described in our previous report [14].

4.8. Hydrolysis of Aldouronic Acid Mixture by TbXyl39A or TbXyl52A Supplemented with TbAgu67A

Hydrolysis of the aldouronic acid mixture was carried out by incubating 400 nM of Xyl39A or 100 nM of Xyl52A individually, or in combination with 200 nM of TbAgu67A, with 1 mg/mL of the aldouronic acid mixture in a total volume of 30 μ L, at 60 °C in the pH 5.5 citrate buffer. The reaction was carried out for 1 h. To minimize variation in results due to evaporation, the reaction products were dried and dissolved in 4 μ L of H₂O. The hydrolysis products were further diluted, centrifuged, and then analyzed by HPAEC using a System Gold high-performance liquid chromatography (HPLC) instrument from Beckman Coulter (Fullerton, CA, USA), equipped with a Coulochem III electrochemical detector from ESA Biosciences (Chelmsford, MA, USA), using X1–X6 as the standards. Details of the methods were outlined in an earlier report [14].

4.9. Identification of Potential Redox-Active and Metal Ion Cofactors for Hemicellulase-Enhancing Oxidoreductases (HEOs)

The potential of TbHEOA and TbHEOB in the synergistic hydrolysis of BWX with the three xylanolytic enzymes (TbXyn10A, TbXyl39A, and TbXyl52A) was analyzed, and potential redox-active cofactors and divalent metal ions were screened. An enzyme mixture composed of five enzymes (10 nM TbXyn10A, 10 nM TbXyl39A, 5 nM TbXyl52A, 50 nM TbHEOA, and 50 nM TbHEOB) was incubated with 5 mg/mL of BWX at 60 °C and pH 5.5 for 16 h, in the presence or absence of different metal ions (1.0 mM Mn²⁺, 1.0 mM Mg²⁺, or 1.0 mM Zn²⁺). The reducing sugars released from the reaction products were measured using the *p*HBAAH method and resolved by TLC, as described above. Based on these results, different potential redox-active cofactors for the two HEOs were screened by incubating the five-enzyme mixture (10 nM TbXyn10A, 10 nM TbXyl39A, 5 nM TbXyl52A, 100 nM TbHEOA, and 100 nM TbHEOB) with 5 mg/mL of BWX at 60 °C, pH 5.5, and 1 mM of metal ion for 16 h, in the presence or absence of different cofactors (1.0 mM of NADH, 1.0 mM of ascorbic acid, or 0.5 mM of reduced glutathione (Re-glu)). The cumulative effects of the screened cofactors and metal ions for the two HEOs on the hydrolysis of BWX with the three xylanolytic enzymes (TbXyn10A, TbXyl39A, and TbXyl52A) were further

examined in the presence of different combinations of the screened cofactors and metal ions. The released reducing ends from these assays were determined using the pHBAH method and further resolved by TLC, as described above.

4.10. Synergistic Effect of the Seven Enzymes in Hydrolyzing Different Xylan-Containing Plant Biomass

The hydrolysis of xylan by all seven enzymes encoded by the hemicellulase gene cluster was carried out at 60 °C and pH 5.5 for 16 h, in the presence of the selected redox-active cofactor and metal ion (1.0 mM of NADH and 1.0 mM of Mn²⁺), by incubation with 5 mg/mL of different substrates (BeeWX, BWX, LWX, OSX, WAX, or Miscanthus). To determine the influence of the different components of the hemicellulose gene cluster, combinations of the seven enzymes (10 nM TbXyn10A, 10 nM TbXyl39A, 5 nM TbXyl52A, 100 nM TbAgu67A, 100 nM TbAxe1A, 50 nM TbHEOA, and 50 nM TbHEOB) were examined for their release of end products from the xylan substrates. The released reducing sugars were determined by the pHBAH method. The components of the reducing sugars were then resolved by TLC and HPLC, as described above.

Supplementary Materials: The following supporting information can be downloaded at: <https://www.mdpi.com/article/10.3390/catal12020182/s1>, Supplemental Table S1: Characteristics that differentiate strain mel9^T from other species of *Thermoanaerobacterium*; Supplemental Table S2: Amino acid sequence identities among the enzymes in the hemicellulase gene clusters from *T. bryantii*, *T. xylanolyticum*, and *T. thermosaccharolyticum*; Supplemental Table S3: End products of synergistic hydrolysis of different xylan-containing plant biomass by the seven enzymes encoded by the *T. bryantii* hemicellulase gene cluster; Supplemental Table S4: Conservations of two adjacent oxidoreductases (TbHEOA and TbHEOB) from *T. bryantii* in other bacteria; Supplemental Table S5: Nucleotide sequences of primers used for cloning of the genes in the hemicellulase gene cluster. Supplemental Figure S1: Hydrolysis of birchwood xylan (BWX) by a single enzyme (TbXyn10A, TbXyl39A, TbXyl52A, TbHEOA, TbHEOB, TbAgu67A, or TbAxe1A) in the gene cluster, as analyzed by the reducing sugar assay; Supplemental Figure S2: Effects of redox-active cofactors and Mn²⁺ ion on the capacity of two new oxidoreductase-like proteins (TbHEOA and TbHEOB) to enhance hydrolysis of BWX by the three-enzyme mixture composed of TbXyn10A, TbXyl39A, and TbXyl52A; Supplemental Figure S3: The synergistic effect of the seven enzymes encoded in the *T. bryantii* hemicellulase gene cluster during hydrolysis of heterogeneous xylans and Miscanthus; Supplemental Figure S4: Multiple sequence alignment of TbHEOA and TbHEOB with three characterized oxidoreductases; Supplemental Figure S5: Multiple sequence alignment of the two HEOs from *T. bryantii* with putative functional homologs occurring as adjacent genes in other bacteria.

Author Contributions: Conceptualization, I.C. and R.I.M.; methodology, I.C., Z.Y., X.S., A.E.A. and P.G.S.; validation, I.C., Z.Y. and X.S.; formal analysis, Z.Y., X.S., A.E.A., A.M.A.-H. and S.C.; investigation, I.C., Z.Y., X.S., A.E.A. and D.D.; resources, I.C. and R.I.M.; data curation, I.C., Z.Y. and X.S.; writing—original draft preparation, I.C., Z.Y., X.S., A.E.A. and A.M.A.-H.; writing—review and editing, I.C., Z.Y., X.S., A.E.A., A.M.A.-H., S.C. and D.D.; supervision, I.C. and R.I.M.; project administration, I.C. and R.I.M.; funding acquisition, I.C. and R.I.M. All authors have read and agreed to the published version of the manuscript.

Funding: This research was supported in part by the Energy Biosciences Institute (EBI) and in part by the Agricultural Experimental Station, university of Illinois, at Urbana-Champaign.

Data Availability Statement: The nucleotide sequences of *tbxyn10A*, *tbagu67A*, *tbheoA*, *tbheoB*, *tbxyl52A*, *tbxyl39A*, and *tbaxe1A* were deposited at the GenBank database with accession numbers JX565592, JX565591, JX565590, JX565589, JX565588, JX565587, and JX565586, respectively.

Conflicts of Interest: The authors declare no conflict of interest.

References

1. Dodd, D.; Cann, I.K. Enzymatic deconstruction of xylan for biofuel production. *Glob. Chang. Biol. Bioenergy* **2009**, *1*, 2–17. [[CrossRef](#)] [[PubMed](#)]
2. Cann, I.; Pereira, G.V.; Abdel-Hamid, A.M.; Kim, H.; Wefers, D.; Kayang, B.B.; Kanai, T.; Sato, T.; Bernardi, R.C.; Atomi, H.; et al. Thermophilic Degradation of Hemicellulose, a Critical Feedstock in the Production of Bioenergy and Other Value-Added Products. *Appl. Environ. Microbiol.* **2020**, *86*, 86. [[CrossRef](#)] [[PubMed](#)]
3. Harris, P.V.; Welner, D.; McFarland, K.C.; Re, E.; Navarro Poulsen, J.C.; Brown, K.; Salbo, R.; Ding, H.; Vlasenko, E.; Merino, S.; et al. Stimulation of lignocellulosic biomass hydrolysis by proteins of glycoside hydrolase family 61: Structure and function of a large, enigmatic family. *Biochemistry* **2010**, *49*, 3305–3316. [[CrossRef](#)] [[PubMed](#)]
4. Beeson, W.T.; Phillips, C.M.; Cate, J.H.D.; Marletta, M.A. Oxidative cleavage of cellulose by fungal copper-dependent polysaccharide monoxygenases. *J. Am. Chem. Soc.* **2011**, *134*, 890–892. [[CrossRef](#)]
5. Langston, J.A.; Shaghasi, T.; Abbate, E.; Xu, F.; Vlasenko, E.; Sweeney, M.D. Oxidoreductive cellulose depolymerization by the enzymes cellobiose dehydrogenase and glycoside hydrolase 61. *Appl. Environ. Microbiol.* **2011**, *77*, 7007–7015. [[CrossRef](#)]
6. Phillips, C.M.; Beeson, W.T.; Cate, J.H.; Marletta, M.A. Cellobiose dehydrogenase and a copper-dependent polysaccharide monoxygenase potentiate cellulose degradation by *Neurospora crassa*. *ACS Chem. Biol.* **2011**, *6*, 1399–1406. [[CrossRef](#)]
7. Quinlan, R.J.; Sweeney, M.D.; Lo Leggio, L.; Otten, H.; Poulsen, J.-C.N.; Johansen, K.S.; Krogh, K.B.R.M.; Jørgensen, C.I.; Tovborg, M.; Anthonsen, A.; et al. Insights into the oxidative degradation of cellulose by a copper metalloenzyme that exploits biomass components. *Proc. Natl. Acad. Sci. USA* **2011**, *108*, 15079–15084. [[CrossRef](#)]
8. Tindall, B.J.; Rosselló-Móra, R.; Busse, H.J.; Ludwig, W.; Kämpfer, P. Notes on the characterization of prokaryote strains for taxonomic purposes. *Int. J. Syst. Evol. Microbiol.* **2010**, *60*, 249–266. [[CrossRef](#)]
9. Wayne, L.G.; Brenner, D.J.; Colwell, R.R.; Grimont, P.A.D.; Kandler, O.; Krichevsky, M.I.; Moore, L.H.; Moore, W.E.C.; Murray, R.G.E.; Stackebrandt, E.; et al. Report of the Ad Hoc Committee on Reconciliation of Approaches to Bacterial Systematics. *Int. J. Syst. Evol. Microbiol.* **1987**, *37*, 463–464. [[CrossRef](#)]
10. Finn, R.D.; Mistry, J.; Schuster-Bockler, B.; Griffiths-Jones, S.; Hollich, V.; Lassmann, T.; Moxon, S.; Marshall, M.; Khanna, A.; Durbin, R.; et al. Pfam: Clans, web tools and services. *Nucleic Acids Res.* **2006**, *34*, D247–D251. [[CrossRef](#)]
11. Kingston, R.L.; Scopes, R.K.; Baker, E.N. The structure of glucose-fructose oxidoreductase from *Zymomonas mobilis*: An osmoprotective periplasmic enzyme containing non-dissociable NADP. *Structure* **1996**, *4*, 1413–1428. [[CrossRef](#)]
12. Whitby, F.G.; Phillips, J.D.; Hill, C.P.; McCoubrey, W.; Maines, M.D. Crystal structure of a biliverdin IX α reductase enzyme–cofactor complex. *J. Mol. Biol.* **2002**, *319*, 1199–1210. [[CrossRef](#)]
13. Thoden, J.B.; Sellick, C.A.; Reece, R.J.; Holden, H.M. Understanding a Transcriptional Paradigm at the Molecular Level. *J. Biol. Chem.* **2007**, *282*, 1534–1538. [[CrossRef](#)]
14. Moon, Y.H.; Iakiviak, M.; Bauer, S.; Mackie, R.I.; Cann, I.K. Biochemical analyses of multiple endoxylanases from the rumen bacterium *Ruminococcus albus* 8 and their synergistic activities with accessory hemicellulose-degrading enzymes. *Appl. Environ. Microbiol.* **2011**, *77*, 5157–5169. [[CrossRef](#)]
15. Sun, H.J.; Yoshida, S.; Park, N.H.; Kusakabe, I. Preparation of (1 \rightarrow 4)-beta-D-xylooligosaccharides from an acid hydrolysate of cotton-seed xylan: Suitability of cotton-seed xylan as a starting material for the preparation of (1 \rightarrow 4)-beta-D-xylooligosaccharides. *Carbohydr. Res.* **2002**, *337*, 657–661. [[CrossRef](#)]
16. Teleman, A.; Tenkanen, M.; Jacobs, A.; Dahlman, O. Characterization of O-acetyl-(4-O-methylglucurono)xylan isolated from birch and beech. *Carbohydr. Res.* **2002**, *337*, 373–377. [[CrossRef](#)]
17. Timell, T.E. Recent progress in the chemistry of wood hemicelluloses. *Wood Sci. Technol.* **1967**, *1*, 45–70. [[CrossRef](#)]
18. Kormelink, F.J.M.; Voragen, A.G.J. Degradation of different [(glucurono)arabino]xylans by a combination of purified xylan-degrading enzymes. *Appl. Microbiol. Biotechnol.* **1993**, *38*, 688–695. [[CrossRef](#)]
19. Vaaje-Kolstad, G.; Westereng, B.; Horn, S.J.; Liu, Z.; Zhai, H.; Sorlie, M.; Eijsink, V.G. An oxidative enzyme boosting the enzymatic conversion of recalcitrant polysaccharides. *Science* **2010**, *330*, 219–222. [[CrossRef](#)]
20. Forsberg, Z.; Vaaje-Kolstad, G.; Westereng, B.; Bunaes, A.C.; Stenstrom, Y.; MacKenzie, A.; Sorlie, M.; Horn, S.J.; Eijsink, V.G. Cleavage of cellulose by a CBM33 protein. *Protein Sci.* **2011**, *20*, 1479–1483. [[CrossRef](#)]
21. Khan, A.W.; Lamb, K.A.; Overend, R.P. Comparison of natural hemicellulose and chemically acetylated xylan as substrates for the determination of acetyl-xylan esterase activity in *Aspergilli*. *Enzyme Microb. Technol.* **1990**, *12*, 127–131. [[CrossRef](#)]
22. Gruppen, H.; Hamer, R.J.; Voragen, A.G.J. Water-unextractable cell wall material from wheat flour. 2. fractionation of alkali-extracted polymers and comparison with water-extractable arabinoxylans. *J. Cereal Sci.* **1992**, *16*, 53–67. [[CrossRef](#)]
23. Somerville, C. Biofuels. *Curr. Biol.* **2007**, *17*, R115–R119. [[CrossRef](#)]
24. Lygin, A.V.; Upton, J.; Dohleman, F.G.; Juvik, J.; Zabolina, O.A.; Widholm, J.M.; Lozovaya, V.V. Composition of cell wall phenolics and polysaccharides of the potential bioenergy crop—*Miscanthus*. *GCB Bioenergy* **2011**, *3*, 333–345. [[CrossRef](#)]
25. Solomon, V.; Teplitsky, A.; Shulami, S.; Zolotnitsky, G.; Shoham, Y.; Shoham, G. Structure-specificity relationships of an intracellular xylanase from *Geobacillus stearothermophilus*. *Acta Crystallogr. D* **2007**, *63*, 845–859. [[CrossRef](#)]
26. Gallardo, Ó.; Pastor, F.I.J.; Polaina, J.; Diaz, P.; Łysek, R.; Vogel, P.; Isorna, P.; González, B.; Sanz-Aparicio, J. Structural insights into the specificity of Xyn10B from *Paenibacillus barcinonensis* and its improved stability by forced protein evolution. *J. Biol. Chem.* **2010**, *285*, 2721–2733. [[CrossRef](#)]

27. Kim do, Y.; Han, M.K.; Oh, H.W.; Bae, K.S.; Jeong, T.S.; Kim, S.U.; Shin, D.H.; Kim, I.H.; Rhee, Y.H.; Son, K.H.; et al. Novel intracellular GH10 xylanase from *Cohnella laeviribosi* HY-21: Biocatalytic properties and alterations of substrate specificities by site-directed mutagenesis of Trp residues. *Bioresour. Technol.* **2010**, *101*, 8814–8821. [[CrossRef](#)]
28. Shi, P.; Tian, J.; Yuan, T.; Liu, X.; Huang, H.; Bai, Y.; Yang, P.; Chen, X.; Wu, N.; Yao, B. *Paenibacillus* sp. strain E18 bifunctional xylanase-glucanase with a single catalytic domain. *Appl. Environ. Microbiol.* **2010**, *76*, 3620–3624. [[CrossRef](#)]
29. Wang, J.; Bai, Y.; Yang, P.; Shi, P.; Luo, H.; Meng, K.; Huang, H.; Yin, J.; Yao, B. A new xylanase from thermoalkaline *Anoxybacillus* sp. E2 with high activity and stability over a broad pH range. *World J. Microb. Biot.* **2010**, *26*, 917–924. [[CrossRef](#)]
30. Zhou, J.; Dong, Y.; Tang, X.; Li, J.; Xu, B.; Wu, Q.; Gao, Y.; Pan, L.; Huang, Z. Molecular and biochemical characterization of a novel intracellular low-temperature-active xylanase. *J. Microbiol. Biotechnol.* **2012**, *22*, 501–509. [[CrossRef](#)]
31. Luthi, E.; Jasmat, N.B.; Bergquist, P.L. Xylanase from the extremely thermophilic bacterium “*Caldocellum saccharolyticum*”: Overexpression of the gene in *Escherichia coli* and characterization of the gene product. *Appl. Environ. Microbiol.* **1990**, *56*, 2677–2683. [[CrossRef](#)] [[PubMed](#)]
32. Lüthi, E.; Love, D.R.; McAnulty, J.; Wallace, C.; Caughey, P.A.; Saul, D.; Bergquist, P.L. Cloning, sequence analysis, and expression of genes encoding xylan-degrading enzymes from the thermophile “*Caldocellum saccharolyticum*”. *Appl. Environ. Microbiol.* **1990**, *56*, 1017–1024. [[CrossRef](#)] [[PubMed](#)]
33. Gallardo, O.; Diaz, P.; Pastor, F.I. Characterization of a *Paenibacillus* cell-associated xylanase with high activity on aryl-xylosides: A new subclass of family 10 xylanases. *Appl. Microbiol. Biotechnol.* **2003**, *61*, 226–233. [[CrossRef](#)] [[PubMed](#)]
34. Taberero, C.; Sanchez-Torres, J.; Perez, P.; Santamaria, R.I. Cloning and DNA sequencing of xyaA, a gene encoding an endo-beta-1,4-xylanase from an alkalophilic *Bacillus* strain (N137). *Appl. Environ. Microbiol.* **1995**, *61*, 2420–2424. [[CrossRef](#)]
35. Dodd, D.; Kiyonari, S.; Mackie, R.I.; Cann, I.K. Functional diversity of four glycoside hydrolase family 3 enzymes from the rumen bacterium *Prevotella bryantii* B14. *J. Bacteriol.* **2010**, *192*, 2335–2345. [[CrossRef](#)]
36. Bravman, T.; Zolotnitsky, G.; Shulami, S.; Belakhov, V.; Solomon, D.; Baasov, T.; Shoham, G.; Shoham, Y. Stereochemistry of family 52 glycosyl hydrolases: A beta-xylosidase from *Bacillus stearothermophilus* T-6 is a retaining enzyme. *FEBS Lett.* **2001**, *495*, 39–43. [[CrossRef](#)]
37. Yang, J.K.; Yoon, H.J.; Ahn, H.J.; Lee, B.I.; Pedelacq, J.D.; Liang, E.C.; Berendzen, J.; Laivenieks, M.; Vieille, C.; Zeikus, G.J.; et al. Crystal structure of b-D-xylosidase from *Thermoanaerobacterium saccharolyticum*, a family 39 glycoside hydrolase. *J. Mol. Biol.* **2004**, *335*, 155–165. [[CrossRef](#)]
38. Withers, S.G. Mechanisms of glycosyl transferases and hydrolases. *Carbohydr. Polym.* **2001**, *44*, 325–337. [[CrossRef](#)]
39. Zachariou, M.; Scopes, R.K. Glucose-fructose oxidoreductase, a new enzyme isolated from *Zymomonas mobilis* that is responsible for sorbitol production. *J. Bacteriol.* **1986**, *167*, 863–869. [[CrossRef](#)]
40. Fujita, Y.; Shindo, K.; Miwa, Y.; Yoshida, K. *Bacillus subtilis* inositol dehydrogenase-encoding gene (idh): Sequence and expression in *Escherichia coli*. *Gene* **1991**, *108*, 121–125.
41. Rossbach, S.; Kulpa, D.A.; Rossbach, U.; de Bruijn, F.J. Molecular and genetic characterization of the rhizopine catabolism (mocABRC) genes of *Rhizobium meliloti* L5-30. *Mol. Gen. Genet.* **1994**, *245*, 11–24. [[CrossRef](#)]
42. Wiebe, M.G.; Nygård, Y.; Oja, M.; Andberg, M.; Ruohonen, L.; Koivula, A.; Penttilä, M.; Toivari, M. A novel aldose-aldose oxidoreductase for co-production of D-xylonate and xylitol from D-xylose with *Saccharomyces cerevisiae*. *Appl. Microbiol. Biotechnol.* **2015**, *99*, 9439–9447. [[CrossRef](#)]
43. Hardman, M.J.; Scopes, R.K. The kinetics of glucose-fructose oxidoreductase from *Zymomonas mobilis*. *Eur. J. Biochem.* **1988**, *173*, 203–208. [[CrossRef](#)]
44. Lee, Y.-E.; Jain, M.K.; Lee, C.; Zeikus, J.G. Taxonomic distinction of saccharolytic thermophilic anaerobes: Description of *Thermoanaerobacterium xylanolyticum* gen. nov., sp. nov., and *Thermoanaerobacterium saccharolyticum* gen. nov., sp. nov.; reclassification of *Thermoanaerobium brockii*, *Clostridium thermosulfurogenes*, and *Clostridium thermohydrosulfuricum* E100-69 as *Thermoanaerobacter brockii* comb. nov., *Thermoanaerobacterium thermosulfurigenes* comb. nov., and *Thermoanaerobacter thermohydrosulfuricus* comb. nov., respectively; and transfer of *Clostridium thermohydrosulfuricum* 39E to *Thermoanaerobacter ethanolicus*. *Int. J. Syst. Bacteriol.* **1993**, *43*, 41–51. [[CrossRef](#)]
45. Liu, S.Y.; Gherardini, F.C.; Matuschek, M.; Bahl, H.; Wiegel, J. Cloning, sequencing, and expression of the gene encoding a large S-layer-associated endoxylanase from *Thermoanaerobacterium* sp. strain JW/SL-YS 485 in *Escherichia coli*. *J. Bacteriol.* **1996**, *178*, 1539–1547. [[CrossRef](#)]
46. Kozianowski, G.; Canganella, F.; Rainey, F.A.; Hippe, H.; Antranikian, G. Purification and characterization of thermostable pectate-lyases from a newly isolated thermophilic bacterium, *Thermoanaerobacter italicus* sp. nov. *Extremophiles* **1997**, *1*, 171–182. [[CrossRef](#)]
47. Larsen, L.; Nielsen, P.; Ahring, B.K. *Thermoanaerobacter mathranii* sp. nov., an ethanol-producing, extremely thermophilic anaerobic bacterium from a hot spring in Iceland. *Arch. Microbiol.* **1997**, *168*, 114–119. [[CrossRef](#)]
48. Ganghofner, D.; Kellermann, J.; Staudenbauer, W.L.; Bronnenmeier, K. Purification and properties of an amylopullulanase, a glucoamylase, and an alpha-glucosidase in the amylolytic enzyme system of *Thermoanaerobacterium thermosaccharolyticum*. *Biosci. Biotechnol. Biochem.* **1998**, *62*, 302–308. [[CrossRef](#)]
49. Warnick, T.A.; Methé, B.A.; Leschine, S.B. *Clostridium phytofermentans* sp. nov., a cellulolytic mesophile from forest soil. *Int. J. Syst. Evol. Microbiol.* **2002**, *52*, 1155–1160. [[CrossRef](#)]

50. StJohn, F.J.; Rice, J.D.; Preston, J.F. *Paenibacillus* sp. Strain JDR-2 and XynA1: A Novel System for Methylglucuronoxylan Utilization. *Appl. Environ. Microbiol.* **2006**, *72*, 1496–1506. [[CrossRef](#)]
51. Foster, B.; Pukall, R.; Abt, B.; Nolan, M.; Glavina Del Rio, T.; Chen, F.; Lucas, S.; Tice, H.; Pitluck, S.; Cheng, J.F.; et al. Complete genome sequence of *Xylanimonas cellulosilytica* type strain (XIL07). *Stand. Genomic Sci.* **2010**, *2*, 1–8. [[CrossRef](#)]
52. Bi, C.; Zhang, X.; Ingram, L.O.; Preston, J.F. Genetic engineering of *Enterobacter asburiae* strain JDR-1 for efficient production of ethanol from hemicellulose hydrolysates. *Appl. Environ. Microbiol.* **2009**, *75*, 5743–5749. [[CrossRef](#)]
53. Khudyakov, J.I.; D'haeseleer, P.; Borglin, S.E.; DeAngelis, K.M.; Woo, H.; Lindquist, E.A.; Hazen, T.C.; Simmons, B.A.; Thelen, M.P. Global transcriptome response to ionic liquid by a tropical rain forest soil bacterium, *Enterobacter lignolyticus*. *Proc. Natl. Acad. Sci. USA* **2012**, *109*, E2173–E2182. [[CrossRef](#)]
54. Piriya, P.S.; Vasanth, P.T.; Padma, V.S.; Vidhyadevi, U.; Archana, K.; Vennison, S.J. Cellulosic ethanol production by recombinant cellulolytic bacteria harbouring *pdc* and *adh II* genes of *Zymomonas mobilis*. *Biotechnol. Res. Int.* **2012**, *2012*, 817549. [[CrossRef](#)]
55. Cann, I.K.; Stroot, P.G.; Mackie, K.R.; White, B.A.; Mackie, R.I. Characterization of two novel saccharolytic, anaerobic thermophiles, *Thermoanaerobacterium polysaccharolyticum* sp. nov. and *Thermoanaerobacterium zeae* sp. nov., and emendation of the genus *Thermoanaerobacterium*. *Int. J. Syst. Evol. Microbiol.* **2001**, *51*, 293–302. [[CrossRef](#)]
56. Mesbah, M.; Premachandran, U.; Whitman, W.B. Precise Measurement of the G + C Content of Deoxyribonucleic Acid by High-Performance Liquid Chromatography. *Int. J. Syst. Bacteriol.* **1989**, *39*, 159–167. [[CrossRef](#)]
57. Arab, H.; Volker, H.; Thomm, M. *Thermococcus aegaicus* sp. nov. and *Staphylothermus hellenicus* sp. nov., two novel hyperthermophilic archaea isolated from geothermally heated vents off Palaeochori Bay, Milos, Greece. *Int. J. Syst. Evol. Microbiol.* **2000**, *50*, 2101–2108. [[CrossRef](#)]
58. Cann, I.K.; Kocherginskaya, S.; King, M.R.; White, B.A.; Mackie, R.I. Molecular cloning, sequencing, and expression of a novel multidomain mannanase gene from *Thermoanaerobacterium polysaccharolyticum*. *J. Bacteriol.* **1999**, *181*, 1643–1651. [[CrossRef](#)]
59. Aziz, R.K.; Bartels, D.; Best, A.A.; DeJongh, M.; Disz, T.; Edwards, R.A.; Formsma, K.; Gerdes, S.; Glass, E.M.; Kubal, M.; et al. The RAST Server: Rapid annotations using subsystems technology. *BMC Genom.* **2008**, *9*, 75. [[CrossRef](#)] [[PubMed](#)]
60. Laemmli, U.K. Cleavage of structural proteins during the assembly of the head of bacteriophage T4. *Nature* **1970**, *227*, 680–685. [[CrossRef](#)] [[PubMed](#)]
61. Lever, M. A new reaction for colorimetric determination of carbohydrates. *Anal. Biochem.* **1972**, *47*, 273–279. [[CrossRef](#)]
62. Dodd, D.; Kocherginskaya, S.A.; Spies, M.A.; Beery, K.E.; Abbas, C.A.; Mackie, R.I.; Cann, I.K.O. Biochemical analysis of a β -D-Xylosidase and a bifunctional xylanase-ferulic acid esterase from a xylanolytic gene cluster in *Prevotella ruminicola* 23. *J. Bacteriol.* **2009**, *191*, 3328–3338. [[CrossRef](#)] [[PubMed](#)]
63. Liu, S.-Y.; Rainey, F.A.; Morgan, H.W.; Mayer, F.; Wiegel, J. *Thermoanaerobacterium aotearoense* sp. nov., a Slightly Acidophilic, Anaerobic Thermophile Isolated from Various Hot Springs in New Zealand, and Emendation of the Genus *Thermoanaerobacterium*. *Int. J. Syst. Bacteriol.* **1996**, *46*, 388–396. [[CrossRef](#)]
64. Jones, D.T.; Woods, D.R. Solvent Production. In *Biotechnology Handbooks. Clostridia*; Minton, N.P., Clarke, D.J., Eds.; Plenum: New York, NY, USA, 1989; Volume 3, pp. 105–144.